Conformation-Dependent • OH/H 2 O 2 Hydrogen Abstraction Reaction Cycles of Gly and Ala Residues: A Comparative Theoretical Study

ARTICLE *in* THE JOURNAL OF PHYSICAL CHEMISTRY B · DECEMBER 2011

Impact Factor: 3.3 · DOI: 10.1021/jp2089559 · Source: PubMed

4 AUTHORS, INCLUDING:

Milán Szőri
University of Szeged
41 PUBLICATIONS **338** CITATIONS
SEE PROFILE

Imre G. Csizmadia
University of Miskolc
534 PUBLICATIONS **7,227** CITATIONS
SEE PROFILE

Béla Viskolcz
University of Miskolc
121 PUBLICATIONS **982** CITATIONS
SEE PROFILE

THE JOURNAL OF PHYSICAL CHEMISTRY B

ARTICLE

pubs.acs.org/JPCB

Conformation-Dependent $^{\bullet}OH/H_2O_2$ Hydrogen Abstraction Reaction Cycles of Gly and Ala Residues: A Comparative Theoretical Study

Michael C. Owen,[†,‡,§,⊥] Milán Szőri,[‡,⊥] Imre G. Csizmadia,[†,‡,§,⊥] and Bela Viskolcz*[,‡,⊥]

[†]Department of Chemistry, University of Toronto, Toronto, Ontario, Canada M5S 3H6

[‡]Department of Chemical Informatics, Faculty of Education, University of Szeged, Boldogasszony sgt. 6, H-6725 Szeged, Hungary

[§]Global Institute of Computational Molecular and Materials Science, Toronto, Ontario, Canada M5S 2K2

[⊥]Drug Discovery Research Center, H-6725 Szeged, Hungary

ABSTRACT: To determine if $^{\bullet}OH$ can initiate the unfolding of an amino acid residue, the elementary reaction coordinates of H abstraction by $^{\bullet}OH$ different conformations (β_L, γ_L, γ_D, α_L, and α_D) of Gly and Ala dimethyl amides were computed using first-principles quantum computations. The MPWKCIS1K/6-311++G-(3df,2p)//BHandHLYP/6-311+G(d,p) level of theory was selected after different combinations of functionals and basis sets were compared. The structures of Gly and Ala in the elementary reaction steps were compared to the conformers of the Gly, Gly$^{\bullet}$, Ala, and Ala$^{\bullet}$ structures in the absence of $^{\bullet}OH/H_2O$, which were identified by optimizing the minima of the respective potential energy surfaces. A dramatic change in conformation is observed in the Gly and Ala conformers after conversion to Gly$^{\bullet}$ and Ala$^{\bullet}$, respectively, and this change can be monitored along the minimal energy pathway. The β_L conformer of Gly (-0.3 kJ mol^{-1}) and Ala (-1.6 kJ mol^{-1}) form the lowest-lying transition states in the reaction with $^{\bullet}OH$, whereas the side chain of Ala strongly destabilizes the α conformers compared to the γ conformers, which could cause the lower reactivity shown in Ala. This effect shown in Ala could affect the abstraction of hydrogen from Ala and the other chiral amino acid residues in the helices. The energy of subsequent hydrogen abstraction reactions between Ala$^{\bullet}$ and Gly$^{\bullet}$ and H_2O_2 remains approximately 90 kJ mol^{-1} below the entrance level of the $^{\bullet}OH$ reaction, indicating that the $^{\bullet}OH$ radical can initiate an α to β transition in an amino acid residue if a molecule such as H_2O_2 can provide the hydrogen atom necessary to re-form Gly and Ala. This work delineates the mechanism of the rapid $^{\bullet}OH$-initiated unfolding of peptides and proteins which has been proposed in Alzheimer's and other peptide misfolding diseases involving amyloidogenic peptides.

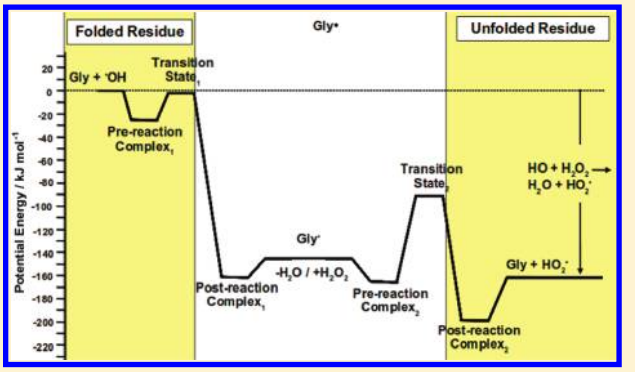

1. INTRODUCTION

Amino acid and peptide and protein radicals have been associated with a wide variety of biological processes and physiological disorders, including aging, Alzheimer's disease, and carcinogenesis.[1−6] Peptide and protein radicals are produced after reactions with free radicals, which are compounds that contain one or more unpaired electrons and are highly reactive.[7,8]

Free radicals can oxidize lipids and DNA and form glycation end products; however, free radicals most frequently react with proteins.[9−12] It has been observed that free radicals destabilize protein structures by causing denaturation, aggregation, fragmentation, and degradation.[13,14] Free radicals can react with peptides and proteins in addition reactions as well as hydrogen abstraction; however, it was shown that abstraction reactions are more prevalent in proteins.[15−18] Free radicals can abstract hydrogen from different amino acid side chains, the amide nitrogen, and C_α of the peptide backbone. The formation of C_α radicals are most frequently observed, primarily because the C_α radical is stabilized by resonance and the "capto-dative" effect, an effect that is strongest when the amino acid residue is in the β conformation.[19−21]

Of the hydrogen abstraction reactions between free radicals and the C_α of amino acid residues, glycyl radicals are the most common and form more frequently than in other residues. This has been observed in electron paramagnetic resonance and radiolysis studies and in the regioselective photoalkylation of peptides and proteins.[15,22−24] C_α-centered glycyl radicals are also used for the enzymatic catalysis displayed by pyruvate formate lyase and ribonucleotide reductase.[25,26] Furthermore, the production of the glycine-extended precursors of peptide hormones by peptidylglycine α-amidating monooxygenase proceeds through a glycyl C_α radical.[27,28] This is in spite of the fact that tertiary radicals should be more stable than secondary radicals.[23,24,29] If this selectivity is due to the presence of two C_α hydrogen atoms available for abstraction, or can be attributed to the ability to form transition states that are lower lying in energy remains to be seen.

Received: September 16, 2011
Revised: December 14, 2011
Published: December 14, 2011

The most reactive free radical of biological relevance is the $^{\bullet}$OH radical. Its half-life in solution is shorter than 10^{-9} s, and it will react with any biological molecule in its vicinity, producing secondary radicals that vary in reactivity.[7,30] It has been shown that $^{\bullet}$OH can be produced by heat or ionization radiation or in several reactions with Fe^{2+}.[30] The relative ease of Gly radical formation compared to that of the other amino acids has been shown thermodynamically, with the stability of the Gly C_α radical product relative to that of the Ala presented as a possible explanation.[31−34] Hydrogen abstraction reactions occur approximately 3 times faster in glycine than in alanine, and it has been proposed that the relative rates of H abstraction from Ala or Gly reflects the ease at which hydrogen can be abstracted from the C_α of the compounds.[31] Moreover, it is believed that the $^{\bullet}$OH radical has less access to the C_α site because of steric hindrance, though the interactions between $^{\bullet}$OH and the side chain of Ala and Gly have not been compared in detail.[31,35] Hydrogen abstraction reactions occur after the formation of a prereaction van der Waals complex. The prereaction complex, stabilized by long-range interactions, has been identified in molecule−radical reactions, including alkenes, haloethanes, aromatic hydrocarbons, and peptides.[36−39] Prereaction complexes can influence the rate of hydrogen abstraction reactions, particularly when the barrier height is close to zero, as in the case of H abstraction reactions with $^{\bullet}$OH.[39]

The presence of the methyl side chain of Ala could be the reason for the difference in the kinetics of hydrogen abstraction reactions between $^{\bullet}$OH and the respective Gly and Ala residues. To see if this is the case, the influence of the methyl side chain of Ala on the stability of the Gly−$^{\bullet}$OH and Ala−$^{\bullet}$OH prereaction complexes, transition states, and postreaction complexes will be determined. This will reveal the extent to which steric hindrance inhibits hydrogen abstraction and also determines which conformations enable or inhibit the progress of the reaction. A similar study revealed the importance of the prereaction complex on H abstraction from Gly in different peptide locations,[40] whereas another study compared the glycine and alanine "free" amino acids.[41] To our knowledge, this is the first report that compares the reaction steps of Gly and Ala used to show the reactivity of Gly in a peptide diamide, a structure that is frequently used to represent the structures of amino acids in a peptide or protein.[33,42,43]

The structures of Gly and Ala residues will be modeled as *N*-methyl-Gly-NHMe (Gly), *N*-methyl-Gly$^{\bullet}$-NHMe (Gly$^{\bullet}$), *N*-methyl-Ala-NHMe (Ala), and *N*-methyl-Ala$^{\bullet}$-NHMe (Ala$^{\bullet}$), which will enable methyl groups to represent the C_α of the neighboring residues, as shown in Figure 1. The Gly$^{\bullet}$ and Ala$^{\bullet}$ diamides will have a C_α-centered radical. Potential energy surfaces (PES) will be used to find the stable conformers of the diamides in the reactants (Gly and Ala), and the products (Gly$^{\bullet}$ and Ala$^{\bullet}$), as shown in Figure 1. These structures will be compared to the structures of the residues in the pre- and postreaction complexes and the respective transition states. We have shown that hydrogen abstraction from the C_α induces the unfolding of Gly and Ala pentapeptides in two previous studies.[44,45] To continue this work, the conformational dependence of the hydrogen abstraction barrier heights will be compared in Gly and Ala residues. Furthermore, the ability of a molecule such as H_2O_2 to convert the Gly$^{\bullet}$ and Ala$^{\bullet}$ radicals to the Gly and Ala residues will be demonstrated and its role in protein unfolding will be discussed.

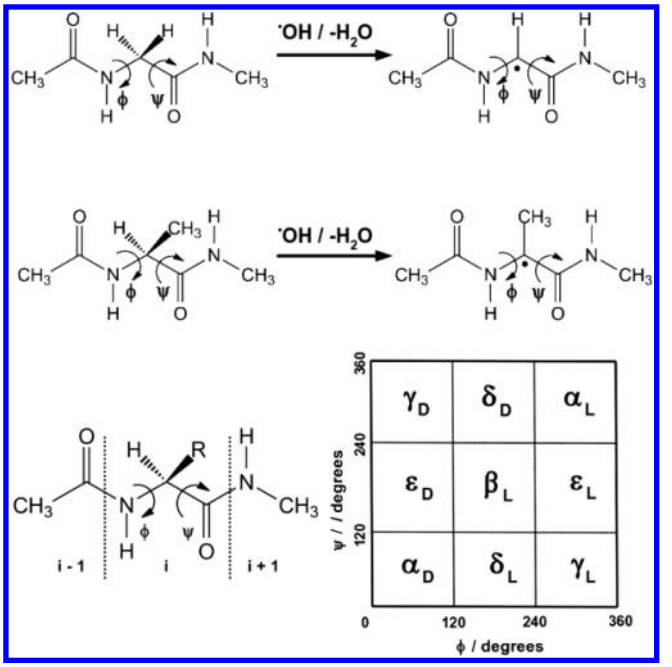

Figure 1. Conformations and corresponding ϕ(C−N−C−C) and ψ(N−C−C−N) dihedral angles used to describe the conformations of the Gly, Gly$^{\bullet}$, Ala, and Ala$^{\bullet}$ amino acid diamides. The *i*, *i* + 1, *i* − 1 residue notation is also defined.

2. METHODS

2.1. Characterizing the Minima and Maxima of the Ala, Ala$^{\bullet}$, Gly, and Gly$^{\bullet}$ Potential Energy Surfaces. All computations were completed with the Gaussian 09 program package.[46] The ϕ and ψ angles of *N*-Ac-Ala-NHMe (Ala), *N*-Ac-Ala$^{\bullet}$-NHMe (Ala$^{\bullet}$), *N*-Ac-Gly-NHMe (Gly), and *N*-Ac-Gly$^{\bullet}$-NHMe (Gly$^{\bullet}$) were rotated in 30° increments to produce 144 conformations for each residue, which were then energy-minimized using the Becke three-parameter Lee−Yang−Parr (B3LYP) density functional, with the 6-31G(d) basis set.[47−49] The potential energies as a function of the ϕ and ψ angles were plotted to construct the potential energy surfaces of Ala, Ala$^{\bullet}$, Gly, and Gly$^{\bullet}$. Each of the minima of the potential energy surfaces was subsequently optimized using the Berny algorithm[50] at the BHandHLYP/6-311+G(d,p) level of theory[51] and were confirmed as such by asserting that none of the calculated frequencies were imaginary. The correction to the standard free energy (G°_{corr}), enthalpy (H°_{corr}), and standard entropy (S°_{corr}) (at T = 298.15 K and P = 1 atm) were also computed at this level of theory. The MPWKCIS1K/6-311++G(3df,2p) level of theory was used to compute the potential energy of the structures.[52] The prereaction and postreaction complexes were found by performing intrinsic reaction coordinate (IRC) calculations in the reverse and forward directions, respectively. An implicit solvent using the conductor-like polarizable continuum model (C-PCM)[53] for water with a dielectric constant of ε = 78.39 was used for all calculations to mimic an aqueous solvent.

The main disadvantage of the self-consistent reaction field (SCRF) method is the absence of explicit water molecules. In an attempt to account for this simplification, the dielectric coefficient is used to account for the "average" of the ensemble of possible hydrogen bonds between the solvent and solutes and to account for the different electrostatic environments that can

Table 1. Activation Energies (T= 298.15 K) of Gly−$^{\bullet}$OH, Ala−$^{\bullet}$OH, Gly$^{\bullet}$−H_2O_2 and Ala$^{\bullet}$−H_2O_2 Calculated with the BHandHLYP and MPWKCIS1K Functionals[a]

		activation energy (ΔE^{o})/kJ mol^{-1}				
transition state	conf	BHandHLYP/ 6-311+G(d,p)	BHandHLYP/ 6-311++G(3df,2p)	G3MP2	MPWKCIS1K/ 6-311+G(d,p)	MPWKCIS1K/ 6-311++G(3df,2p)
Gly-$^{\bullet}$OH	β_L	12.2	−5.3	−2.9	0.2	−0.3
	γ_L	18.1	0.1	2.2	4.5	3.8
	γ_D	15.1	−4.2	5.7	1.0	0.3
	α_L	22.2	4.2	3.4	7.9	7.0
	α_D	19.9	1.1	7.5	6.6	5.6
Ala-$^{\bullet}$OH	β_L	11.0	−6.4	−6.3	−1.3	−1.6
	γ_L	14.0	−3.7	−3.1	2.1	1.6
	γ_D	19.1	0.4	0.6	3.8	2.9
	α_L	15.2	−3.0	−4.2	2.7	1.8
	α_D	20.4	2.4	5.9	9.6	8.6
Gly$^{\bullet}$-H_2O_2	β_L	57.3	51.8	44.9	45.8	51.2
Ala$^{\bullet}$-H_2O_2	β_L	35.1	47.6	31.9	41.4	47.8
MAD		19.4 (19.4)	15.7 (9.9)	0.0 (0.0)	9.5 (6.9)	15.9 (6.0)
AAD		14.5 (15.8)	4.2 (2.7)	0.0 (0.0)	4.2 (4.0)	4.8 (3.6)

[a] The G3MP2 method was used as a reference. The maximum absolute deviation (MAD) and average absolute deviation (AAD) are reported, and the deviations pertaining to the Gly−$^{\bullet}$OH and Ala−$^{\bullet}$OH transition states are in parentheses.

surround a peptide when exposed to water. Previous benchmark calculations indicate that the BHandHLYP functional yields geometries that are in good agreement with results obtained by high-level (G3MP2B3) ab initio methods, which in turn give results that are in excellent agreement with experimentally derived results in radical systems.[40,54−57] Moreover, the MPWKCIS1K functional yields hydrogen abstraction barrier-height energy values that are in excellent agreement with G3MP2B3 ab initio methods.[58] Several transition states involving Gly, Gly•, Ala, and Ala• with $^{\bullet}$OH and H_2O_2 were computed in this study. The ability of the MPWKCIS1K and BHandHLYP functionals to reproduce the activation energies computed with the G3MP2B3 method was compared by using the 6-311+G(d,p) and 6-311++G(3df,2p) basis sets. The results of this comparison are discussed in section 3.1. The use of the SCRF with these functionals should yield acceptable results in the systems studied herein.

The relative energy values of the structures will be discussed throughout, whereas the temperature-dependent parameters ΔG^{o}, ΔH^{o}, and ΔS^{o} will be presented for comparison. This will enable the temperature-independent results obtained herein to be compared to larger systems, with more degrees of freedom.

3. RESULTS

3.1. Comparison of the MPWKCIS1K and BHandHLYP functionals. Activation energies of Gly−$^{\bullet}$OH, Ala−$^{\bullet}$OH, Gly$^{\bullet}$−H_2O_2, and Ala$^{\bullet}$−H_2O_2 transition states using the BHandHLYP/6-311+G(d,p), BHandHLYP/6-311++G(3df,2p), MPWKCIS1K/6-311+G(d,p), and MPWKCIS1K/6-311++G(3df,2p) methods were calculated on geometries obtained by the BHandHLYP/6-311+G(d,p) level of theory. The G3MP2//BHandHLYP/6-311G(d,p) calculations[55,58] were used as a reference, and the results of the comparison are shown in Table 1. The maximum absolute deviation (MAD) and average absolute deviation (AAD) of the BHandHLYP/6-311+G(d,p) energies from the reference values are 19.4 and 14.5 kJ mol^{-1}, respectively, showing that the use of this functional with the smaller basis set is unsuitable for computing transition state energies, given the overestimation of the activation energies. The use of the BHandHLYP/6-311++G(3df,2p) (MAD = 15.7 kJ mol^{-1}, AAD = 4.2 kJ mol^{-1}), MPWKCIS1K/6-311+G(d,p) (MAD = 9.5 kJ mol^{-1}, AAD = 4.2 kJ mol^{-1}) and MPWKCIS1K/6-311++G(3df,2p) (MAD = 15.9 kJ mol^{-1}, AAD = 6.0 kJ mol^{-1}) functionals yielded results that are close to experimental error, given that the AAD values are 6.0 kJ mol^{-1} or less.

The use of either basis set with the MPWKCIS1K functional and the larger basis set with the BHandHLYP functional are suitable for these systems. When the reaction involving OH is combined with that of H_2O_2 to regenerate Gly or Ala, the Gly−$^{\bullet}$OH and Ala−$^{\bullet}$OH transition states were shown to be the rate-limiting step. Therefore, the accuracy of the Gly−$^{\bullet}$OH and Ala−$^{\bullet}$OH barrier height energies are crucial for determining the minimum energy path for the $^{\bullet}$OH-initiated unfolding of Gly and Ala. When the conformers of the Gly−$^{\bullet}$OH and Ala−$^{\bullet}$OH transition states are considered, the MAD and AAD obtained from the MPWKCIS1K/6-311++G(3df,2p) combine to be the lowest of the three methods (MAD = 6.0 kJ mol^{-1}, AAD = 3.6 kJ mol^{-1}), and, therefore, this method was chosen for the remainder of the calculations. The efficiency of this computational method makes it suitable for use in larger systems in future studies.

3.2. Gly, Gly$^{\bullet}$, Ala, and Ala$^{\bullet}$ Potential Energy Surfaces. Figure 2 shows the Gly and Ala potential energy surfaces. The subsequent optimization of the minima of the PES of Gly and Ala each yielded five minima: β_L, γ_L, γ_D, α_L, and α_D. The β_L conformer is the global minimum in the case of Gly, whereas the α_L conformer is the global minimum of the Ala PES. The ϕ and ψ angles and energy values for all of the minima can be found in Table 2. In Ala, the D-conformers are more than 10 kJ mol^{-1} higher in energy than the respective L-conformers. Conversely, in Gly, the L-configurations of the α and γ conformers are identical to their respective D-configuration.

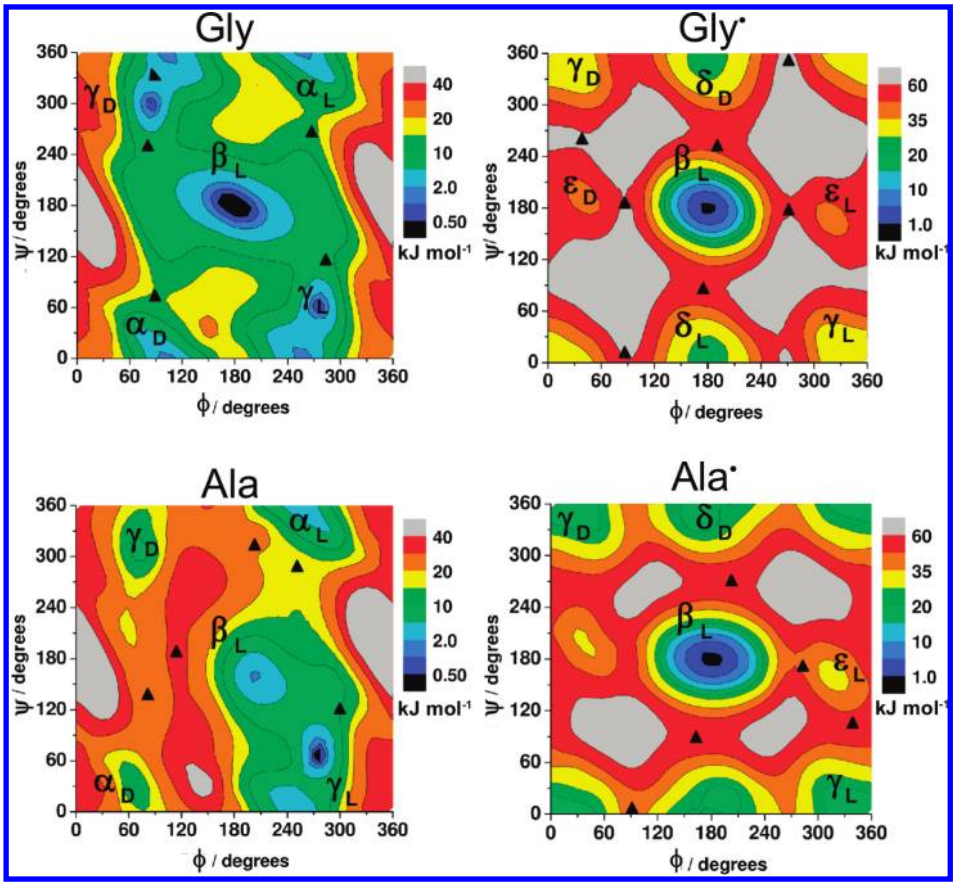

Figure 2. Potential energy surfaces of the Gly, Gly•, Ala, and Ala• amino acid diamides. The minima are labeled by their respective conformation whereas the transition states are labeled with triangles.

The β_L conformer is the global minimum of both the Ala• and the Gly• potential energy surfaces. These structures have the lowest relative free energy and enthalpy, and also have the most entropy. In contrast to the closed-shell Gly and Ala potential energy surfaces, the other minima in the Gly• and Ala• surfaces are much higher in energy (>18 kJ mol^{-1}) than their respective global minimum. The energies of the less stable minima of Gly• are greater than the global minimum by 20 kJ mol^{-1}, whereas energies of the Ala• minima are 15 kJ mol^{-1} higher in energy than the global minimum. Moreover, to convert from the global minima of the Gly• and Ala• structures to any of the other minima requires at least 50 kJ mol^{-1} of energy to overcome the ϕ and ψ rotational barriers. Therefore, the Gly• and Ala• peptide radicals are prone to convert to the β_L conformer. This increased barrier height can be attributed to the increased electron delocalization and increased influence of the capto-dative effect shown in the β_L conformation and constrains the conformation of the Gly and Ala structures in the β-conformation. The first-order saddle points of the potential energy surfaces listed in Table 2 show the relative flexibility of the Gly Gly•, Ala, and Ala• residues. The difference in energy between the minima and first-order saddle points of Gly (17 kJ mol^{-1}) is less than that of Ala (33 kJ mol^{-1}), indicating that Gly is more flexible than Ala. The relative energy of the first-order saddle point of the Gly• PES is similar to those of Ala and Ala•, suggesting that the peptide radicals have a similar flexibility. The ΔH° values corresponded well with the electronic energy values (ΔE). The ΔG° values were usually more elevated than the ΔE values, and this increase was usually coupled to an increase in the negativity of the ΔS° value. The ΔS° values of the transition states were generally lower than those of the minima, due to the extra intrinsic degree of freedom of the TS structures.

3.3. Gly and Ala van der Waals Prereaction Complexes. In each Gly van der Waals complex, the hydrogen atom of the •OH radical formed a hydrogen bond with a carbonyl oxygen that was between 1.73 and 1.80 Å (Table 4). The structures of the van der Waals complexes are shown in Figure 3. In the γ_D and α_D conformations, the hydrogen atom formed a hydrogen bond with the carbonyl residue of the *i*th residue, whereas the oxygen atom of the •OH radical was equidistant from both the pro-L and pro-D hydrogen atoms. This was also true for the β_L conformation; however, the hydroxyl hydrogen formed a hydrogen bond to the carbonyl carbon of residue "$i-1$". The γ_L and α_L Gly complexes were the highest in energy, in spite of the fact that the distance between the hydroxyl oxygen and the pro-D hydrogen was the shortest in these structures. The β_L and α_D conformations of Gly were the most stable van der Waals complexes. The relative energies of the prereaction complexes are listed in Table 3, whereas the complex-formation energy values are listed in Table 5. The γ_L conformation formed the prereaction complex that was the highest in energy. A relatively large ΔS° contributed to the stability of the γ_D conformation.

In the Ala α_D prereaction complex the carbonyl oxygen of residues i and $i-1$ were too far from the pro-D hydrogen to enable a hydrogen bond to form with the hydrogen atom of the hydroxyl radical. This is shown in Figure 4. As such, this

Table 2. Conformation, ϕ and ψ Angles, Intraresidue Hydrogen Bond [(N)H···O(=C)] and the ΔE^{o}_{rel}, ΔG^{o}_{rel}, ΔH^{o}_{rel}, ΔS^{o}_{rel} (298.15 K, 1 atm) of the Lowest Energy Conformations and Transition-State Structures of Gly, Gly$^{\bullet}$, Ala, and Ala$^{\bullet}$[a]

struct	conf	ϕ, ψ/deg	(N)H···O(=C)/Å	ΔE^{o}_{rel}/kJ mol^{-1}	ΔG^{o}_{rel}/kJ mol^{-1}	ΔH^{o}_{rel}/kJ mol^{-1}	ΔS^{o}_{rel}/J mol^{-1} K^{-1}
Gly	β_L	−179.9, 179.9	2.18	0.0	0.0	0.0	0.0
	γ_L	−83.9, 60.4	2.06	3.8	9.5	5.2	−14.6
	γ_D	83.9, −60.4	2.06	3.8	9.5	5.2	−14.6
	α_L	−92.5, −5.8	3.37	0.1	−0.1	0.7	2.9
	α_D	92.6, 5.6	3.37	0.1	−0.1	0.7	2.8
[Gly]‡	$\gamma_D \leftrightarrow \alpha_D$	88.0, 6.70	3.19	2.8	5.4	−1.1	−21.8
	$\beta_L \leftrightarrow \gamma_L$	−77.4, −115.2	2.78	11.5	16.8	8.1	−29.3
	$\beta_L \leftrightarrow \gamma_D$	77.4, 115.2	2.78	11.5	16.8	8.1	−29.2
	$\beta_L \leftrightarrow \alpha_L$	−95.3, −74.2	3.97	16.4	20.3	12.7	−25.4
	$\beta_L \leftrightarrow \alpha_D$	95.2, 74.2	3.97	16.4	20.3	12.7	−25.4
Gly$^{\bullet}$	β_L	−179.9, −180.0	2.3	0.0	0.0	0.0	0.0
	γ_L	−20.4, 4.6	1.81	31.0	31.8	31.9	0.5
	γ_D	20.2, −4.8	1.81	30.9	32.5	31.9	−2.0
	δ_L	−172.8, 12.4	3.87	39.3	40.3	38.4	−6.3
	δ_D	172.8, −12.4	3.87	21.0	23.9	21.0	−9.7
	ε_L	−47.2, 165.9	3.73	39.3	40.3	38.4	−6.3
	ε_D	47.2, −165.9	3.73	39.3	40.3	38.4	−6.3
[Gly$^{\bullet}$]‡	$\gamma_L \leftrightarrow \delta_D$	10.7, −94.1	3.07	61.8	63.9	57.0	−23.1
	$\delta_L \leftrightarrow \gamma_D$	−95.5, −2.2	3.35	57.2	53.2	50.2	−10.0
	$\delta_D \leftrightarrow \gamma_L$	95.5, 2.2	3.35	57.2	53.2	50.2	−10.1
	$\beta_L \leftrightarrow \delta_L$	165.1, 97.5	3.21	54.2	54.7	49.4	−17.9
	$\beta_L \leftrightarrow \delta_D$	−165.2, −97.5	3.21	54.2	54.7	49.4	−17.8
	$\beta_L \leftrightarrow \varepsilon_L$	−86.0, 178.4	3.16	59.1	55.7	52.3	−11.2
	$\beta_L \leftrightarrow \varepsilon_D$	86.0, −178.4	3.16	59.1	55.7	52.3	−11.2
Ala	β_L	−154.3, 156.7	2.23	0.0	0.0	0.0	0.0
	γ_L	−85.8, 70.5	2.09	1.3	4.0	1.8	−7.3
	γ_D	74.4, −52.6	1.93	10.5	16.3	11.7	−15.4
	α_L	−83.0, −17.6	3.36	−0.7	0.4	−0.3	−2.4
	α_D	63.7, 34.1	3.21	9.6	12.3	9.7	−8.8
[Ala]‡	$\beta_L \leftrightarrow \alpha_L$	−96.7, −75.3	3.92	15.8	16.0	10.4	−18.7
	$\beta_L \leftrightarrow \gamma_L$	−76.4, 117.6	2.88	7.5	8.6	2.4	−20.8
	$\alpha_D \leftrightarrow \gamma_D$	81.5, 155.4	3.24	25.5	28.2	26.0	−21.5
	$\beta_L \leftrightarrow \gamma_D$	117.4, −150.4	2.32	33.5	36.7	29.0	−25.7
	$\alpha_L \leftrightarrow \gamma_D$	−157.6, −61.1	3.50	19.6	20.5	14.1	−21.5
Ala$^{\bullet}$	β_L	−171.9, 176.8	2.09	0.0	0.0	0.0	0.0
	γ_L	−46.7, 10.8	1.85	18.3	22.0	18.0	−13.5
	γ_D	46.7, −10.7	1.85	18.3	22.0	18.0	−13.6
	ε_L	−48.8, 159.5	4.28	24.0	26.8	22.8	−13.4
	δ_D	155.5, −15.0	3.75	15.5	20.7	15.3	−18.2
[Ala$^{\bullet}$]‡	$\beta_L \leftrightarrow \delta_L$	−13.5, 96.1	3.03	45.5	48.5	39.8	−29.2
	$\beta_L \leftrightarrow \delta_L$	95.7, 2.6	3.32	30.8	28.9	23.1	−19.7
	$\beta_L \leftrightarrow \delta_L$	−84.3, 172.7	3.04	40.2	37.4	32.7	−15.6
	$\beta_L \leftrightarrow \delta_L$	−177.3, 99.9	2.95	53.2	54.1	47.8	−21.4
	$\beta_L \leftrightarrow \delta_L$	177.3, −99.9	2.95	53.2	54.1	47.8	−21.4

[a] The transition states are identified by the minima to which they are connected.

van der Waals complex was the least stable. The hydrogen atom of the hydroxyl radical formed a hydrogen bond with the residue *i* carbonyl carbon of γ_D and α_L; however, the α_L van der Waals complex was the lowest in energy. The β_L van der Waals complex formed a 9-membered ring, linking the carbonyl oxygen of residue $n - 1$ to the amide hydrogen of residue $n + 1$. The hydrogen bond within residue *i* remained intact.

3.4. Gly and Ala Transition States. The hydrogen atom of the $^{\bullet}$OH radical formed a hydrogen bond with the carbonyl carbon of the $i - 1$ residue of Gly in the transition state when Gly was in the β_L, γ_L, and α_L conformations. The structures of the transition states are shown in Figure 3. The β_L conformer of Gly was the lowest-lying transition state, whereas the γ_L and α_L conformations had the highest energy. The $^{\bullet}$OH radical completed a

dx.doi.org/10.1021/jp2089559 |J. Phys. Chem. B 2012, 116, 1143–1154

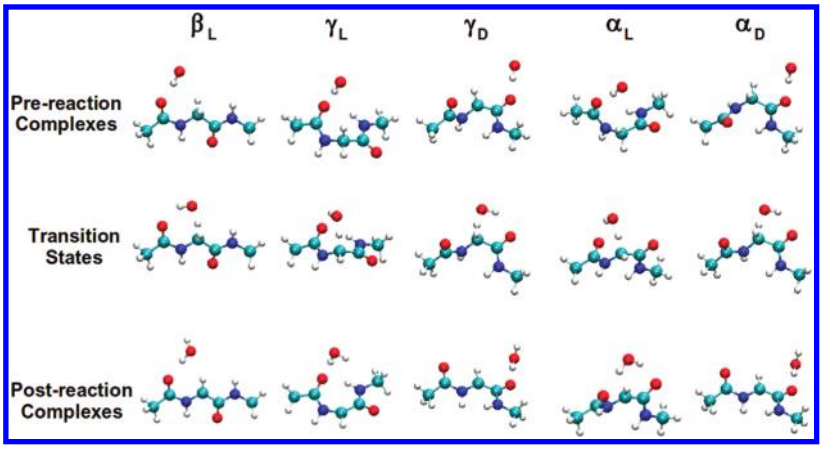

Figure 3. Prereaction van der Waals complexes, transition states, and postreaction complexes for the hydrogen abstraction from Gly by $^{\bullet}$OH. The distances between the $^{\bullet}$OH/H_2O molecule and each conformation of the Gly/Gly$^{\bullet}$ diamide are shown in Table 4.

Table 3. ϕ and ψ Angles, Relative Potential Energy, ΔE^{o}_{rel}, ΔG^{o}_{rel}, ΔH^{o}_{rel}, and ΔS^{o}_{rel} (298.15 K, 1 atm) for Each of the Gly and Ala Prereaction and Postreaction Complexes and Transition States with the $^{\bullet}$OH Radical[a]

struct	conf	ϕ, ψ/deg	ΔE^{o}/kJ mol^{-1}	ΔG^{o}/kJ mol^{-1}	ΔH^{o}/kJ mol^{-1}	ΔS^{o}/J mol^{-1} K^{-1}
Gly−OH prereaction complex	β_L	178.3, −176.9	0.0	0.0	0.0	0.0
	γ_L	−85.1, 50.7	10.4	11.2	9.4	−6.2
	γ_D	94.1, 4.0	0.8	2.8	14.0	37.8
	α_L	−92.2, −4.0	2.7	3.2	2.6	−2.0
	α_D	93.4, 5.0	−0.9	−2.5	−0.9	−5.4
[Gly···$^{\bullet}$OH]‡	β_L	−174.4, −170.8	0.0	0.0	0.0	0.0
	γ_L	−76.2, 46.5	10.9	12.8	11.0	−6.2
	γ_D	140.4, −25.1	7.5	5.9	7.5	0.7
	α_L	−75.7, −11.3	10.7	10.7	10.1	0.2
	α_D	140.4, −25.1	7.5	5.9	7.5	7.1
Gly postreaction complex	β_L	−179.7, −179.9	0.0	0.0	0.0	0.0
	γ_L	−35.4, 5.0	35.7	35.6	20.1	−52.0
	γ_D	172.7, −13.2	16.5	19.3	18	−4.4
	α_L	−51.0, −27.4	39.1	37.1	22.8	−47.8
	α_D	172.6, −12.9	16.6	12.9	0.9	−40.4
Ala−OH prereaction complex	β_L	−155.7, 156.9	0.0	0.0	0.0	0.0
	γ_L	−85.8, 69.0	5.7	−3.8	−10.3	−21.8
	γ_D	74.0, −55.1	9.0	−1.7	9.4	37.6
	α_L	−80.2, −21.5	−0.5	−11.8	−16.2	−14.9
	α_D	64.7, 33.2	32.5	15.9	31.3	51.7
[Ala···$^{\bullet}$OH]‡	β_L	−160.5, 175.9	0.0	0.0	0.0	0.0
	γ_L	−78.4, 52.2	4.8	5.7	4.7	−3.4
	γ_D	78.1, −58.2	3.6	2.7	3.8	−3.6
	α_L	−58.4, −38.4	22.3	15.1	20.7	−18.6
	α_D	64.9, 32.6	20.6	19.1	19.9	2.9
Ala postreaction complex	β_L	−170.2, 176.8	0.0	0.0	0.0	0.0
	γ_L	−53.5, 9.9	20.6	27.0	4.0	−77.3
	γ_D	45.5, −14.0	16.1	26.6	15.3	−37.8
	α_L	−58.2, −25.1	22.9	22.1	21.0	−3.7
	α_D	56.8, 18.6	14.7	19.8	14.5	−17.9

[a] The β_L conformation was the reference conformation for each structure.

seven-membered ring by forming a bridge between the $i-1$ carbonyl and the C_α hydrogen atom. Conversely, the hydroxyl oxygen formed a hydrogen bond of the ith carbonyl carbon, and therefore formed a six-membered ring in the transition state when the Gly residue was in the γ_D and α_D conformations. The transition states that formed six-membered rings were lower in

dx.doi.org/10.1021/jp2089559 |J. Phys. Chem. B 2012, 116, 1143–1154

Table 4. Distances between the Gly and Ala Diamide and the OH Radical along the Reaction Coordinate[a]

		distances/Å		
struct	conf	C···H(−O)	(C−)H···O	H···O(=C)
Gly−OH prereaction complex	β_L	1.087	3.161	1.733
	γ_L	1.085	3.052	1.770
	γ_D	1.084	3.630	1.803
	α_L	1.082	2.915	1.754
	α_D	1.084	3.634	1.727
[Gly···•OH]‡	β_L	1.200	1.347	2.114
	γ_L	1.216	1.316	2.111
	γ_D	1.209	1.330	2.170
	α_L	1.226	1.292	2.059
	α_D	1.209	1.329	2.169
Gly−H_2O postreaction complex	β_L	2.268	–	1.841
	γ_L	1.892	–	1.899
	γ_D	4.676	–	1.803
	α_L	2.997	–	1.946
	α_D	4.680	–	1.803
Ala−OH prereaction complex	β_L	1.084	2.934	1.731
	γ_L	1.084	2.536	–
	γ_D	1.081	3.018	1.719
	α_L	1.084	3.252	1.726
	α_D	1.086	2.453	5.188
[Ala···•OH]‡	β_L	1.206	1.339	2.015
	γ_L	1.207	1.332	2.063
	γ_D	1.225	1.272	2.077
	α_L	1.207	1.334	2.162
	α_D	1.200	1.338	4.026
Ala−H_2O postreaction complex	β_L	5.156	–	1.845
	γ_L	3.800	–	1.886
	γ_D	4.361	–	1.805
	α_L	3.180	–	1.913
	α_D	1.913	–	1.91

[a] The C···H(−O) bond is between the C_α and the hydrogen (to be abstracted) the (C−)H···O bond is between the abstracted hydrogen and the oxygen of the hydroxyl group and the H···O(=C) bond is between the hydroxyl oxygen and the carbonyl carbon of the amino acid diamide.

Table 5. ΔE^o and ΔG^o (298.15 K, 1 atm) of the Prereaction Complexes, Transition States, and Postreaction Complexes Relative to the Those of the Reactants of the Hydrogen Abstraction Reactions from Gly and Ala by •OH and the Subsequent Abstraction of Hydrogen from H_2O_2 by Gly• and Ala•

		ΔE^o (ΔG^o)/kJ mol^{-1}			
reaction	conf	prereaction complex	transition state	postreaction complex	products
Gly + •OH → Gly• + H_2O	β_L	−24.5 (9.2)	−0.3 (32.9)	−159.8 (−124.0)	−144.7 (−148.0)
	γ_L	−19.0 (10.9)	3.8 (36.2)	−127.9 (−98.0)	
	γ_D	−29.4 (2.5)	0.3 (29.3)	−147.1 (−118.8)	
	α_L	−21.4 (12.5)	7.0 (43.7)	−120.7 (−86.9)	
	α_D	−25.5 (6.9)	5.6 (38.9)	−143.3 (−110.9)	
Ala + •OH → Ala• + H_2O	β_L	−24.4 (19.6)	−1.6 (32.4)	−156.4 (−128.3)	−141.7 (−148.8)
	γ_L	−19.9 (11.8)	1.6 (34.1)	−137.1 (−105.3)	
	γ_D	−25.9 (23.2)	2.9 (35.2)	−152.3 (−124.8)	
	α_L	−24.1 (7.4)	1.8 (34.7)	−139.6 (−102.2)	
	α_D	−1.4 (23.1)	8.6 (35.2)	−143.1 (−118.5)	
Gly• + H_2O_2 → Gly + HO_2•	β_L	−23.3 (9.3)	51.2 (94.8)	−53.3 (−2.1)	−15.9 (−11.1)
Ala• + H_2O_2 → Ala + HO_2•	β_L	−23.1 (18.5)	47.8 (101.7)	−55.9 (−5.1)	−18.8 (−10.3)

dx.doi.org/10.1021/jp2089559 |J. Phys. Chem. B 2012, 116, 1143–1154

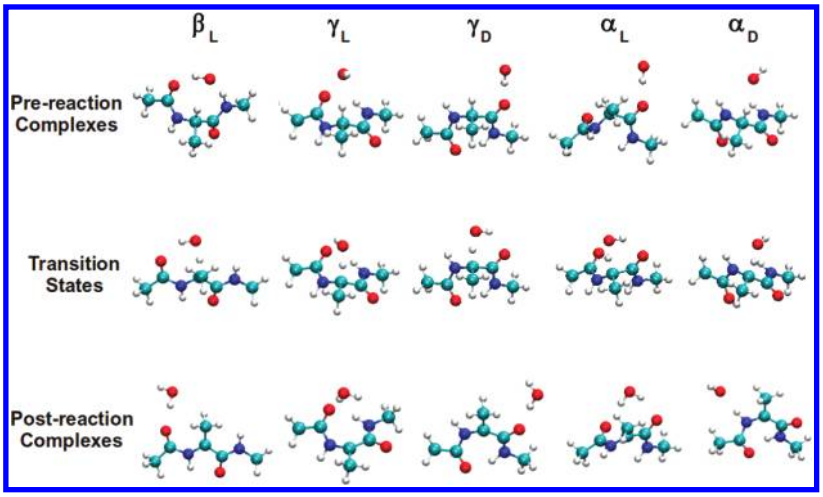

Figure 4. Prereaction van der Waals complexes, transition states, and postreaction complexes for the hydrogen abstraction from Ala by $^{\bullet}$OH. The distances between the $^{\bullet}$OH/H_2O molecule and each conformation of the Ala/Ala$^{\bullet}$ diamide are shown in Table 4.

energy than those that are composed of a seven-membered ring. The relative stabilities of the transition states are reported in Table 3.

Six-membered rings were formed in the α_L and γ_D conformations of the transition state between the $^{\bullet}$OH radical and Ala. However, the α_L transition state was lower-lying, and this is probably due to the hydrogen bond that formed between the $i-1$ carbonyl oxygen and $i+1$ amide hydrogen. The structures of the Ala transition states are also shown in Figure 3. The steric hindrance caused by the methyl group of Ala prevented the formation of ring structures for the α_D transition state. The hydrogen of the $^{\bullet}$OH radical may be interacting with the amide nitrogen in the case of the α_D conformation, since the distance between these atoms is approximately 3.4 Å. These values can be found in Table 4. The β_L transition state was the lowest-lying Ala transition state, whereas the α_D and α_L were the highest in energy. The $\Delta E°$, $\Delta G°$, and $\Delta H°$ values were in close agreement for the transition states of both residues.

3.5. Gly and Ala Postreaction Complexes. The water molecule that forms after the hydrogen atom is abstracted from Gly$^{\bullet}$ forms a hydrogen bond between 1.80 and 1.95 Å in length with a carbonyl carbon. These values are listed in Table 4. The γ_D and α_D transition states formed the same van der Waals complex, with ϕ and ψ angles close to 173° and −13°, respectively, and their conformation is similar to that of the γ_D conformation observed in the Gly$^{\bullet}$ in the absence of H_2O. The relative energy of this van der Waals complex (16.5 kJ mol^{-1}, Table 3) is also similar to that of the γ_D conformation of the Gly$^{\bullet}$ (21.0 kJ mol^{-1}, Table 2), indicating that the H_2O molecule has a small effect on the relative stabilities of the complexes. Both the relative energies and ϕ and ψ angles are shown in Table 3. However, the γ_L and α_L transition states (35.7 and 39.1 kJ mol^{-1}) converged to van der Waals complexes that were similar in structure to the γ_L conformation of Gly$^{\bullet}$. The β_L van der Waals complex was the lowest in energy and the ϕ and ψ angles of the Gly$^{\bullet}$ were −179.7° and −179.9°, respectively. The water molecule in the Gly$^{\bullet}$ complexes stabilized the α_L and α_D conformations more than the others.

The β_L postreaction van der Waals complex of Ala$^{\bullet}$ with water was the lowest in energy. The ϕ and ψ angles of the complex were −170.2° and 176.8°, respectively, which deviated slightly from the ϕ and ψ angles of Ala$^{\bullet}$ in the absence of water, (−171.9° and 176.7°). The γ_L and α_L conformations were similar in energy, whereas the γ_D and α_D conformations were similar to each other in energy, and lower in energy than the γ_L and α_L conformations. This energy difference can be attributed to the orientation of the water molecule. One of the hydrogen atoms of H_2O formed a hydrogen with the amide nitrogen in the α_D conformer of Ala. However, this water orientation was also observed in the β_L conformation, which was the lowest in energy. The closest distance between the oxygen of the water molecule and the carbon of the Ala side chain is 3.62 and 3.64 Å in the α_L and γ_D conformations, respectively.

3.6. Gly and Ala H Abstraction Reaction Coordinates. Table 5 contains the energy of the prereaction van der Waals complex, hydrogen abstraction transition state, and postreaction complex for each of the conformations of Gly, Gly$^{\bullet}$, Ala, and Ala$^{\bullet}$. The energy values are relative to the sum of the energies of the respective Gly and Ala conformation and an infinitely separated $^{\bullet}$OH radical. The relative energy of the prereaction van der Waals complexes of Gly were between −19.0 and −29.4 kJ mol^{-1}, whereas the Ala values were between −1.4 and −25.9 kJ mol^{-1}. The formation of the γ_D prereaction complex of Gly was the most favorable. Moreover, the γ_D and α_D conformations of the Gly prereaction complexes were lower in energy than the respective γ_L and α_L conformations. The γ_L and α_D prereaction complexes of Ala were the highest in energy.

The β_L conformations of Gly and Ala were the lowest-lying transition states, which were approximately 1 kJ mol^{-1} lower in energy than the respective conformation of the reactant and the $^{\bullet}$OH radical. All of the other transition states had positive activation energies. The α_L transition state of Ala and the γ_D transition state of Gly were the next lowest-lying of the respective structures, and were within 3 kJ mol^{-1} of the β_L energy. The β_L conformation of Gly$^{\bullet}$ postreaction complex was the lowest in energy, which was approximately 11 kJ mol^{-1} higher in energy than that of the γ_D conformation, which had the second highest relative energy. Inter-residue comparison shows that the relative stability of the β_L postreaction complex of Gly$^{\bullet}$ was only 2.4 kJ mol^{-1} higher in energy than the β_L conformation of the Ala$^{\bullet}$ postreaction complex, which had the lowest energy of the Ala$^{\bullet}$ complexes.

dx.doi.org/10.1021/jp2089559 |J. Phys. Chem. B 2012, 116, 1143–1154

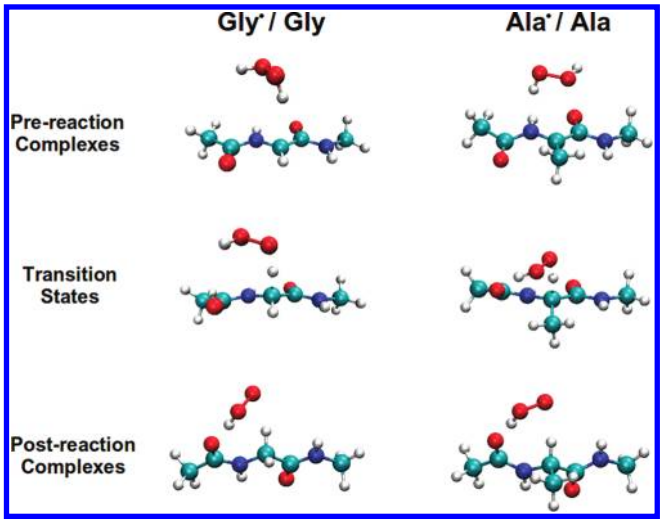

Figure 5. Prereaction van der Waals complexes, transition states, and postreaction complexes for the hydrogen abstraction from H_2O_2 by Gly• and Ala•.

Given the relative energy of the β_L conformation of Gly• and Ala• in the absence of H_2O, the sum of the energies of the respective structures in the β_L conformation and that of H_2O was used to represent the energy of the dissociated products, which was -144.7 kJ mol^{-1} for Gly• + H_2O and -141.7 kJ mol^{-1} for Ala• + H_2O. The β_L, γ_D, and van der Waals complexes are lower in energy than the dissociated Gly• and H_2O, whereas the γ_L, α_L, and α_D complexes are not. In the case of Ala•, the β_L, α_D, and γ_D complexes are lower in energy than the dissociated Ala• and H_2O, whereas the γ_L and α_L were higher in energy than the dissociated Ala• and H_2O. The complexes in which H_2O formed two hydrogen bonds with the Gly or Ala residue, as in the case of the γ_L and α_L conformations, were the least stable, as these complexes had ϕ and ψ angles that deviated the most from the corresponding ϕ and ψ angles of the respective Gly• and Ala• residues.

3.7. Hydrogen Abstraction by Gly• and Ala• Radicals from H_2O_2. After being chemically activated by the •OH radical, the formation of Gly• and Ala• radicals from the Gly and Ala residues resulted in -144.7 and -141.7 kJ mol^{-1} to be released in the case of Gly and Ala, respectively. The formation of the Gly•$-H_2O_2$ and Ala•$-H_2O_2$ prereaction complexes released -23.3 kJ mol^{-1} in the case of Gly• and -23.1 kJ mol^{-1} for Ala•, as shown in Table 5. The transition-state energies of Gly• and Ala• were also similar; however, the Gly transition state was approximately 5 kJ mol^{-1} higher than that of Ala. The geometries of the Ala• and Gly• transition-state structures are shown in Figure 5. An eight-membered ring was formed between H_2O_2 and Ala•. A similar structure was observed for the Gly residue; however, the distance between the carbonyl carbon and H_2O_2 molecule was 0.9 Å larger in the Gly transition state. Moreover, the postreaction Ala van der Waals complex and the infinitely separated Ala and HO_2• were lower in energy than the respective Gly structures by 2.6 and -2.9 kJ mol^{-1}, respectively. The postreaction van der Waals structures of both Gly and Ala were both lower in energy than the respective noninteracting products.

During the reaction in which H_2O_2 regenerates Gly, the energy stays well below the energy of the entrance level, which is the sum of the energies of •OH and the Gly residue. This is shown in Figure 6. The transition state of the hydrogen abstraction reaction between Gly• and H_2O_2 is approximately 90 kJ mol^{-1} lower in energy than the energy of the entrance level, which suggests that the subsequent reaction with H_2O_2 can take place following activation by •OH.

4. DISCUSSION

4.1. Gly and Ala Prereaction van der Waals Complexes. The differences between the relative energies of the Gly and Ala prereaction complexes show that the Ala side chain could inhibit the formation of the γ_D and α_D prereaction complexes. The relative energies of the β_L, γ_D, α_L, and α_D prereaction complexes of Gly are within 4 kJ mol^{-1} of each other, whereas the γ_L is a slight outlier, which suggests that the prereaction complex can form easily from multiple conformations. The distribution of the prereaction Ala energy values are similar; however, the α_D and γ_D complexes are higher in energy. It is worth noting that the α_D prereaction complex is only 1.4 kJ mol^{-1} lower than the energy at the entrance level. The side chain of the Ala residue destabilizes this complex by hindering the ability of the oxygen atom of the •OH radical to form a hydrogen bond with the pro-D hydrogen of the Ala residue. As a result, the formation energy of the complex in this conformation is 20−25 kJ mol^{-1} less than the other conformations. The complex-formation energies of all five conformations of Gly and the four (excluding α_D) of Ala indicate that the formation energies of the prereaction complexes are sufficient enough to enable the hydrogen abstraction reaction to occur, particularly when the activation energy is close to zero.[37,59] When these nine conformations of the residues are considered, the formation energies of the prereaction complexes show that the Ala side chain does not significantly inhibit complex formation. Side chains larger than Ala could further hinder complex formation, and a future study could provide a rationale for this effect.

With the exception of the γ_D conformation of Gly, the ϕ and ψ angles of the Gly and Ala van der Waals complexes are within a few degrees of the ϕ and ψ angles of the respective Gly and Ala residues. Therefore, these complexes can form without perturbing the structure of the respective Gly and Ala minima, and the differences in relative energy only depend on the interaction between the •OH radical and the respective residues. This can also be expected if explicit water molecules were studied as well, since the •OH would occupy a similar place that a structural H_2O molecule would occupy. The lack of conformational change of the residues during complex formation with OH enables the H-abstraction reaction to occur with greater ease.

4.2. Gly and Ala Transition-State Structures. Both Gly and Ala combine with •OH to form six- and seven-membered rings in the respective transition-state structures. The ϕ and ψ angles of the Gly transition-state structures remain similar to those of the Gly PES, whereas the ψ angle of γ_D becomes more like the ψ angle of Gly•. The change in the conformation of Ala the β_L transition state suggests that the capto-dative stabilization of Ala in this conformation is less than that of Gly, and is likely to be the reason for the decreased relative energy of the Ala β_L transition state. It can be concluded that the transition states of each conformation of the Gly and Ala residues except for the γ_D of Gly and β_L of Ala deviate from the geometries of the PES minima by only a few degrees.

Both the Gly and Ala transition states in the β_L conformation are below the entrance level, and the next lowest lying transition

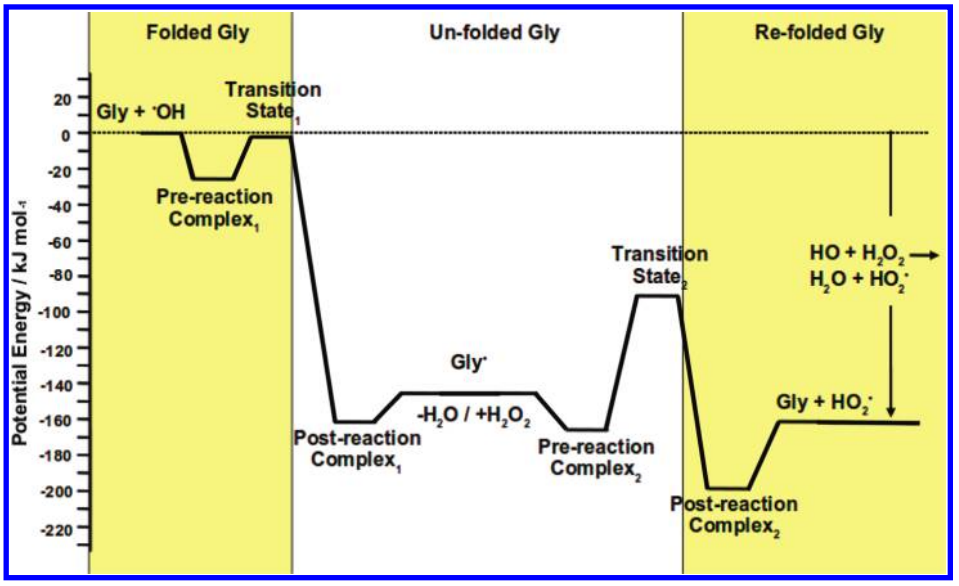

Figure 6. Potential energy diagram showing the E_{pot} of the hydrogen abstraction from Gly in the β_L conformation by $^{\bullet}$OH (reaction 1) and the subsequent hydrogen abstraction from H_2O_2 by Gly$^{\bullet}$ and Ala$^{\bullet}$ in the β_L conformation (reaction 2). The sum of the energies of Gly and OH is used as a reference, which shows that energy of the two reactions stays below the energy of the entrance level.

states of Gly are the γ_D and α_D conformations, followed by the γ_L and α_L conformations. The ϕ and ψ angles indicate that the β_L conformation is capto-dative stabilized, and is the reason for the low-lying β_L conformation; however, the differences between the energy of the other conformations are less significant. After the β_L conformation, the next lowest lying transition states of Ala are the γ_L and γ_D, followed by the α_L and α_D transition states which are much higher in energy. The Ala side chain has a larger influence on the energy of these conformations, and a distinct conformational effect can be observed in Ala.

4.3. Gly and Ala Postreaction van der Waals Complexes with H_2O. The relative energy values of the Gly and Ala postreaction van der Waals complexes were similar to those of the respective Gly$^{\bullet}$ and Ala$^{\bullet}$ PES minima. The geometries of the postreaction complexes only varied from the fully isolated Gly$^{\bullet}$ and Ala$^{\bullet}$ residues by a few degrees, except for the α_L complex of Gly and Ala, which are not similar to any of the respective Gly$^{\bullet}$ or Ala$^{\bullet}$ conformations. Moreover, the corresponding α_D conformation of Gly$^{\bullet}$ converged to the γ_D, which can be attributed to the absence of the methyl group of the Ala side chain. The postreaction complexes of the Gly$^{\bullet}$ residue were more planar than the respective Ala$^{\bullet}$ complex, which is probably due to the increased capto-dative stabilization of the Gly residue. The H_2O molecule interacts with the Gly$^{\bullet}$ and Ala$^{\bullet}$ with a hydrogen bond between a hydrogen atom of water and one of the carbonyl oxygen atoms. In the γ_L and α_L complexes of Gly$^{\bullet}$ and the γ_L of Ala$^{\bullet}$ hydrogen bonds form with both carbonyl oxygen atoms, but these complexes are the highest in energy.

The postreaction complexes of Gly are 120.7−159.8 kJ mol^{-1} below the energy of the entrance level, and those of Ala are 137.1−156.4 kJ mol^{-1} below the Ala entrance level. This complex is the lowest point of the reaction coordinate for both the Gly and Ala residue, and the stabilities of these complexes show that their formation is a significant driving force for the progress of the H abstraction reactions. The side chain of Ala does not appear to interact with the H_2O molecule, and the stability of the complex is largely influenced by the hydrogen

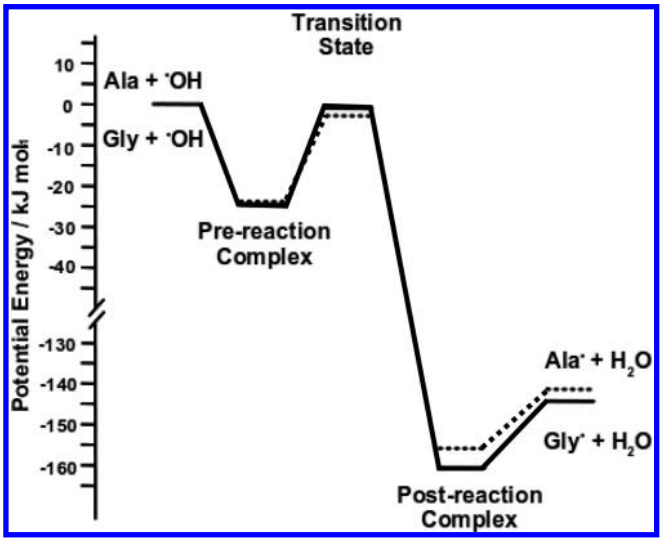

Figure 7. Potential energy diagram showing the E_{pot} of the hydrogen abstraction from Gly and Ala in the β_L conformation by $^{\bullet}$OH. The energy of the reactants is used as a reference.

bond between the water molecule and the residue and the ϕ and ψ angles of the residue. This is supported by the observation that these angles remain similar to those of the respective Gly and Ala residues in the absence of the H_2O molecule. The ϕ and ψ angles of Gly and Ala are expected be similar if this system were to include structural water.

4.4. Hydrogen Abstraction by Gly$^{\bullet}$ and Ala$^{\bullet}$ Radicals from H_2O_2. To compare the stability of the C_α-centered radical of Gly$^{\bullet}$ and Ala$^{\bullet}$, we also compared the relative energies for the hydrogen abstraction from H_2O_2 by Gly$^{\bullet}$ and Ala$^{\bullet}$, in order to form the Gly and Ala residues. H_2O_2 can donate a hydrogen atom and can be found in areas of the body where $^{\bullet}$OH can be found as well. It should be stressed that H_2O_2 is not the only molecule that can play this role, but it has been selected as an example.

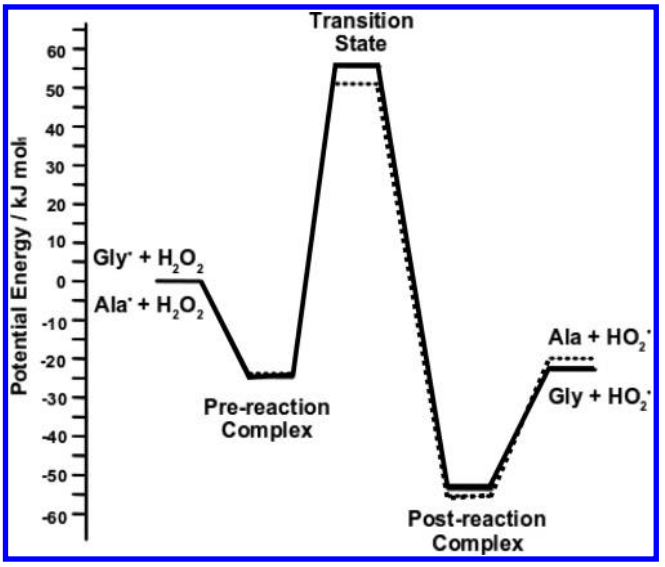

Figure 8. Potential energy diagram showing the E_{pot} of the hydrogen abstraction from H_2O_2 by Gly$^\bullet$ and Ala$^\bullet$ in the β_L conformation. The energy of the reactants is used as a reference.

The β_L conformation of these residues was used as the starting conformation because they are the lowest in energy, as shown in the potential energy surfaces (Figure 2). Both the Gly and Ala residues are likely to unfold to the β conformer following hydrogen abstraction from any of the other conformers. The formation energy of the van der Waals complex is the same for both residues; however, the lower lying transition state and subsequent van der Waals complex and separated products of the Ala residue show that the Ala$^\bullet$ would be easier to convert back to Ala, whereas the Gly$^\bullet$ would have a higher propensity to remain a C_α radical, as shown in Figure 7. A representative scheme of the reaction coordinate for the reformation of Gly and Ala can be found in Figure 8.

Since the energies of the Gly$-^\bullet$OH/Gly$^\bullet-H_2O_2$ and Ala$-^\bullet$OH/Ala$^\bullet-H_2O_2$ systems remain below the energy of the entrance level, the re-formation to Gly and Ala by H_2O_2 has enough energy to proceed. Using Gly as an example, it has been shown that the postreaction complexes contain Gly in the β_L, γ_L, and δ_D conformations, whereas the Gly$^\bullet$ PES indicated that other Gly$^\bullet$ minima are stable. However, the relative energy values of Gly$^\bullet$ PES minima indicate that the β_L conformation is approximately 30 kJ mol^{-1} more stable. This can also be said for Ala and presumably for any other residue. This suggests that any rearrangement of the residue will result in the residue converting to the β_L conformation. These results can help elucidate the mechanism by which $^\bullet$OH initiates protein unfolding, and potentially aggregate. It would be interesting to see if the conversion to the β_L conformer that was shown here can be reproduced using other techniques, particularly molecular dynamics, which enables the time-dependent nature of this unfolding to be observed in larger systems.

5. CONCLUSIONS

The PES for the Gly, Gly$^\bullet$, Ala, and Ala$^\bullet$ structures show the stable conformers for these residues. The Gly and Ala PES each contained five minima, which remained similar to the geometries of the respective prereaction complexes and transition states. Changes to the ϕ and ψ angles were shown upon the formation of the postreaction complexes, which were similar to the structures of the Gly$^\bullet$ and Ala$^\bullet$ conformers. The first-order saddle points of the PES showed that the Gly residue loses its flexibility when changed to Gly$^\bullet$, whereas the flexibilities of Ala and Ala$^\bullet$ are similar.

The stability of the β_L conformer of Gly and Ala radicals was shown in transition state and postreaction van der Waals complex with the $^\bullet$OH radical. The β_L conformer of the Gly and Ala radicals is stabilized by resonance and the capto-dative effect and it is suspected that these factors also influence the stability of the transition state and van der Waals complexes. The γ and α conformers of the Gly transition state were of similar energy, whereas the Ala side chain strongly destabilized the α conformers of the transition-state structures. This could inhibit the abstraction of hydrogen from residues other than glycyl in helical peptides and proteins. Given the similarity between the structures of H_2O and $^\bullet$OH, the structure of the complexes found herein should be similar to the structure of these complexes in the presence of structural water.

The unfolded Gly$^\bullet$ and Ala$^\bullet$ residues can be converted to Gly and Ala by H_2O_2 (as an example), since the energy of the system remains well below the pre-$^\bullet$OH abstraction entrance. The conversion of Gly and Ala to the β conformer shown in this work reveals a possible mechanism for the $^\bullet$OH-initiated unfolding of peptides and proteins.

AUTHOR INFORMATION

Corresponding Author

*E-mail: viskolcz@jgypk.u-szeged.hu. Phone: (36-62) 544720. Fax: (36-62) 420953.

ACKNOWLEDGMENT

We thank László Müller and Máté Labádi for the administration of the computing systems used for this work. This work was supported by the project TÁMOP-4.2.1/B-09/1/KONV-2010-0005—Creating the Center of Excellence at the University of Szeged which is supported by the European Union and cofinanced by the European Regional Fund. This work was supported by the Faculty Grant CS-007/2010.

REFERENCES

(1) Cohen, S. M. *Environ. Health Perspect.* **1983**, *50*, 51–59.
(2) Kobliashev, V. A. *Biochemistry (Moscow)* **2010**, *75*, 675–685.
(3) Fatehi-Hassanabad, Z.; Chan, C. B.; Furman, B. L. *Eur. J. Pharmacol.* **2010**, *636*, 8–17.
(4) Jenner, P. *Ann. Neurol.* **2003**, *53* (Suppl 3), S26–S36.
(5) Barnham, K. J.; Masters, C. L.; Bush, A. I. *Nat. Rev. Drug Discov.* **2004**, *3*, 205–214.
(6) Stadtman, E. R. *Free Radical Res.* **2006**, *40*, 1250–1258.
(7) Valko, M; Izakovic, M; Mazur, M; Rhodes, C. J.; Telser, J. *J. Mol. Cell Biochem.* **2004**, *266*, 37–56.
(8) Wolff, S. P.; Dean, R. T. *Biochem. J.* **1986**, *234*, 399–403.
(9) Spiteller, G. *Free Radical Biol. Med.* **2006**, *41*, 362–387.
(10) Dizdaroglu, M. *Mutat. Res.* **1992**, *275*, 331–342.
(11) Fu, M. X.; Wells-Knecht, K. J.; Blackedge, J. A.; Lyons, T. J.; Thorpe, S. R.; Baynes, J. W. *Diabetes* **1994**, *43*, 676–683.
(12) Gebicki, J. M.; Nauser, T.; Domazou, A.; Steinmann, D.; Bounds, P. L.; Koppenol, W. H. *Amino Acids* **2010**, *39*, 1131–1137.
(13) Davies, K. J. A. *J. Biol. Chem.* **1987**, *262*, 9895–9901.
(14) Willix, R. L.; Garrison, W. M. *Radiat. Res.* **1967**, *32*, 452–462.
(15) Garrison, W. M. *Chem. Rev.* **1987**, *87*, 381–398.

(16) Garrison, W. M.; Jayco, M. E.; Bennett, A. *Radiat. Res.* **1962**, *16*, 483–502.
(17) Swallow, A. J. *Radiation Chemistry of Organic Compounds*; John Wiley & Sons: New York, 1960.
(18) Schuessler, H.; Schilling, K. *Int. J. Radiat. Biol.* **1983**, *45*, 267–281.
(19) Viehe, H. G.; Merenyi, R.; Stella, L.; Janousek, Z. *Angew. Chem., Int. Ed. Engl.* **1979**, *18*, 917–932.
(20) Baldock, R. W.; Hudson, P.; Katritzky, A. R.; Soti, F. *Heterocycles* **1973**, *1*, 67.
(21) Baldock, R. W.; Hudson, P.; Katritzky, A. R.; Soti, F. *J. Chem. Soc., Perkin Trans. 1* **1974**, 1422–1427.
(22) Hawkins, C. L; Davies, M. J. *J. Chem. Soc., Perkin Trans.* **1998**, *2*, 2617–2622.
(23) Sperling, J.; Elad, D. *J. Am. Chem. Soc.* **1971**, *93*, 3839–3840.
(24) Schwarzberg, M.; Sperling, J.; Elad, D. *J. Am. Chem. Soc.* **1973**, *95*, 6418–6426.
(25) Becker, A.; Fritz-Wolf, K.; Kabsch, W.; Knappe, J.; Schultz, S.; Wagner, A. F. V. *Nat. Struct. Biol.* **1999**, *6*, 969–975.
(26) Logan, D. T.; Andersson, J.; Sjöberg, B. -M.; Nordlund, P. *Science* **1999**, *283*, 1499–1504.
(27) Prigge, S. T.; Kolhekar, A. S.; Eipper, B. A.; Mains, R. E.; Amzel, L. M. *Science* **1997**, *278*, 1300–1305.
(28) Prigge, S. T.; Kolhekar, A. S.; Eipper, B. A.; Mains, R. E.; Amzel, L. M. *Nat. Struct. Biol.* **1999**, *6*, 976–983.
(29) Russell, G. A. In *Free Radicals*; Kochi, J. K., Ed.; Wiley, New York, 1973; Vol. 1, p 275.
(30) Halliwell, B.; Gutteridge, M. C. *Biochem. J.* **1984**, *219*, 1–14.
(31) Easton, C. J.; Hay, M. P. *J. Chem. Soc. Chem. Commun.* **1986**, 55–57.
(32) Burgess, V. A.; Easton, C. J.; Hay, M. P. *J. Am. Chem. Soc.* **1989**, *111*, 1047–1057.
(33) Rauk, A.; Armstrong, D. A.; Fairlie, D. P. *J. Am. Chem. Soc.* **2000**, *122*, 9761–9767.
(34) Rauk, A.; Armstrong, D. A. *J. Am. Chem. Soc.* **2000**, *122*, 4185–4192.
(35) Easton, C. J. *Chem. Rev.* **1997**, *97*, 53–82.
(36) Alvarez-Idaboy, J. R.; Díaz-Acosta, I.; Vivier-Bunge, A. J. *J. Comput. Chem.* **1998**, *88*, 811–819.
(37) Sekusak, S.; Sabljic, A. *Chem. Phys. Lett.* **1997**, *272*, 353–360.
(38) Uc, V. H.; García-Cruz, I.; Hernández-Laguna, A.; Vivier-Bunge, A. *J. Phys. Chem.* **2000**, *104*, 7847–7855.
(39) Lin, R.-J.; Wu, C.-C.; Jang, S.; Li, F.-Y. *J. Mol. Model.* **2010**, *16*, 175–182.
(40) Lu, H.-F.; Li, F.-Y.; Lin, S. H. *J. Comput. Chem.* **2007**, *28*, 783–794.
(41) Galano, A.; Alvarez-Idaboy, J. R.; Montero, L. A.; Vivier-Bunge, A. *J. Comput. Chem.* **2001**, *22*, 1138–1153.
(42) Owen, M. C.; Komáromi, I.; Murphy, R. F.; Lovas, S. *J. Mol. Struct.* **2006**, *759*, 117–124.
(43) Zhu, X.; Koenig, P.; Hoffmann, M.; Yethiraj, A.; Cui, Q. *J. Comput. Chem.* **2010**, *31*, 2063–2077.
(44) Owen, M. C.; Viskolcz, B.; Csizmadia, I. G. *J. Phys. Chem. B.* **2011**, *115*, 8014–8023.
(45) Owen, M. C.; Viskolcz, B.; Csizmadia, I. G. *J. Chem. Phys.* **2011**, *135*, 035101.
(46) Frisch, M. J., et al. *Gaussian 09*; Gaussian Inc: Wallingford, CT, 2009.
(47) Becke, A. D. *Phys. Rev. A* **1988**, *38*, 3098–3100.
(48) Becke, A. D. *J. Chem. Phys.* **1996**, *104*, 1040–1046.
(49) Lee, C.; Yang, W.; Parr, R. G. *Phys. Rev. B* **1988**, *37*, 785–789.
(50) Li, X.; Frisch, M. J. *J. Chem. Theory Comput.* **2006**, *2*, 835–839.
(51) Note that BHandHLYP means $0.5E_X^{HF} + 0.5E_X^{LSDA} + 0.5\Delta E_X^{Becke88} + E_C^{LYP}$ functional.
(52) Zhao, Y.; González-García, N.; Truhlar, D. G. *J. Phys. Chem. A* **2005**, *109*, 2012–2018.
(53) Cossi, M.; Rega, N.; Scalmani, G.; Barone, V. *J. Comput. Chem.* **2002**, *24*, 669–681.
(54) Wille, U. *J. Org. Chem.* **2006**, *71*, 4040–4048.
(55) Szőri, M.; Fittschen, C.; Csizmadia, I. G.; Viskolcz, B. *J. Chem. Theory Comput.* **2006**, *2*, 1575–1586.
(56) Szőri, M.; Abou-Abdo, T.; Fittschen, C.; Csizmadia, I. G.; Viskolcz, B. *Phys. Chem. Chem. Phys.* **2007**, *9*, 1931–1940.
(57) Janoscheck, R.; Rossi, M. *Int. J. Chem. Kinet.* **2002**, *34*, 550–560.
(58) Fiser, B.; Szőri, M.; Jójárt, B.; Izsák, R.; Viskolcz, B.; Csizmadia, I. G. *J. Phys. Chem. B.* **2011**, *115*, 11269–11277.
(59) Alvarez-Idaboy, J. R.; Mora-Diez, N.; Boyd, R. J.; Vivier-Bunge, A. *J. Am. Chem. Soc.* **2001**, *123*, 2018–2024.